

IMPROVED OBJECT CLASSIFICATION ACCURACY THROUGH THE COMBINATION OF VNIR, MULTI-FREQUENCY SAR AND MULTI-POLARMETRIC SAR: A case study from South Australia

David BRUCE

Director, Spatial Measurement and Information Group,
University of South Australia,
GPO Box 2471, City East Campus, Adelaide, South Australia, 5001
Tel: (61)-8-302-1856 Fax: (61)-8-83022252
E-mail: david.bruce@unisa.edu.au
AUSTRALIA

KEY WORDS: Classification, SAR, Visible, Infrared, Accuracy, Image, Fusion.

ABSTRACT

This paper extends the suggestion by Bruce (2000), that image classification accuracy can be increased by the addition of co-registered synthetic aperture radar (SAR) imagery to visible and near infrared (VNIR) imagery. The paper examines the increase in classification accuracy through the addition of C, L and P band SAR to Landsat TM7 VNIR imagery. The multi-spectral SAR is further extended through multi-polarization backscatter measured in the TOPSAR mode of the JPL AIRSAR instrument flown in PACRIM 2000. The test site for the study, which is located east of Adelaide in South Australia, features rolling topography with land use ranging from horticulture, viticulture, pasture, crops and irrigated agriculture through to native forestry. The 2000 AIRSAR data capture occurred at a 5m spatial resolution providing a DTM (from C band interferometry) and polarimetric imagery in L and P bands (VV, HH and HV) and VV polarization imagery at C band. Using detailed land use maps and additional field data as ground truth, a supervised classification of each of the image types was conducted and classification accuracy computed. The VNIR component of the ETM⁺ imagery was merged with the higher resolution ETM⁺ panchromatic imagery to produce imagery of 12.5m spatial resolution. The TOPSAR image, after geometric and radiometric calibration, was classified using the same training areas as for the VNIR imagery. TOPSAR data was then resampled to 12.5m and merged with Landsat ETM⁺ imagery. The merged imagery was classified using the same training areas as utilized for the earlier classifications. Classifications of VNIR together with C and L band and then with P band imagery proceeded. Classification accuracies were computed for all images and combinations. Results showed significant improvement in classification accuracy when C and L band wavelengths were processed together with VNIR. The addition of P band, whilst improving the classification accuracy, did not do so significantly.

BACKGROUND

Bruce (2000) has demonstrated the potential for improved vegetation discrimination from the combination of Landsat TM5 VNIR imagery with JERS L band SAR imagery. In this work vegetation discrimination improved as a result of the detection of object structural properties via backscatter at L band (23cm wavelength) with HH polarization. The vegetation focused upon was that of grape vines which were grown upon wood and wire trellises the support structures of which provided double bounce return to the SAR antenna. When combined with the spectral reflectance in the visible and near infrared part of the electromagnetic spectrum this scattering enabled discrimination between irrigated summer crops / pastures and grape vines. The objective in this prior research, which was to increase the classification accuracy for mapping grape vines from satellite image data, was achieved. There was no attempt to increase the number of classified objects beyond the class of grape vines and other objects. However, the work inferred that the classification accuracy of other classes of objects could be improved.

The opportunity to test the hypothesis that the combination of VNIR and SAR can improve object classification accuracy came as a result of the PACRIM 2 AIRSAR mission. This airborne SAR, built and operated by JPL and NASA visited many sites across and around the Pacific Rim during 2000 (see <http://airsar.jpl.nasa.gov/cgi-bin/internet.plex?year=2000&uid=>) The AIRSAR aircraft was based in Adelaide, South Australia for many of the southern Australian sites and acquired imagery over several test sites in the Mount Lofty Ranges, near Adelaide, in August 2000. VNIR imagery of the same area was available from Landsat earlier in 2000 and thus an opportunity to advance the classification of fused

imagery existed. A simultaneous acquisition of hyperspectral MASTER data with the TOPSAR data proved unsuccessful due to poor weather conditions.

RESEARCH OBJECTIVES

In order to test the hypothesis declared above a test site with known ground truth was required. Such a site was available from previous work (Bruce *et al*, 1999) and was located in the central Mount Lofty Ranges east of Adelaide, the capital city of South Australia (see Figure 1). Part of the site had been imaged in 1993 by the AIRSAR sensor with the focus of that research being in the area of soil moisture and soil degradation.

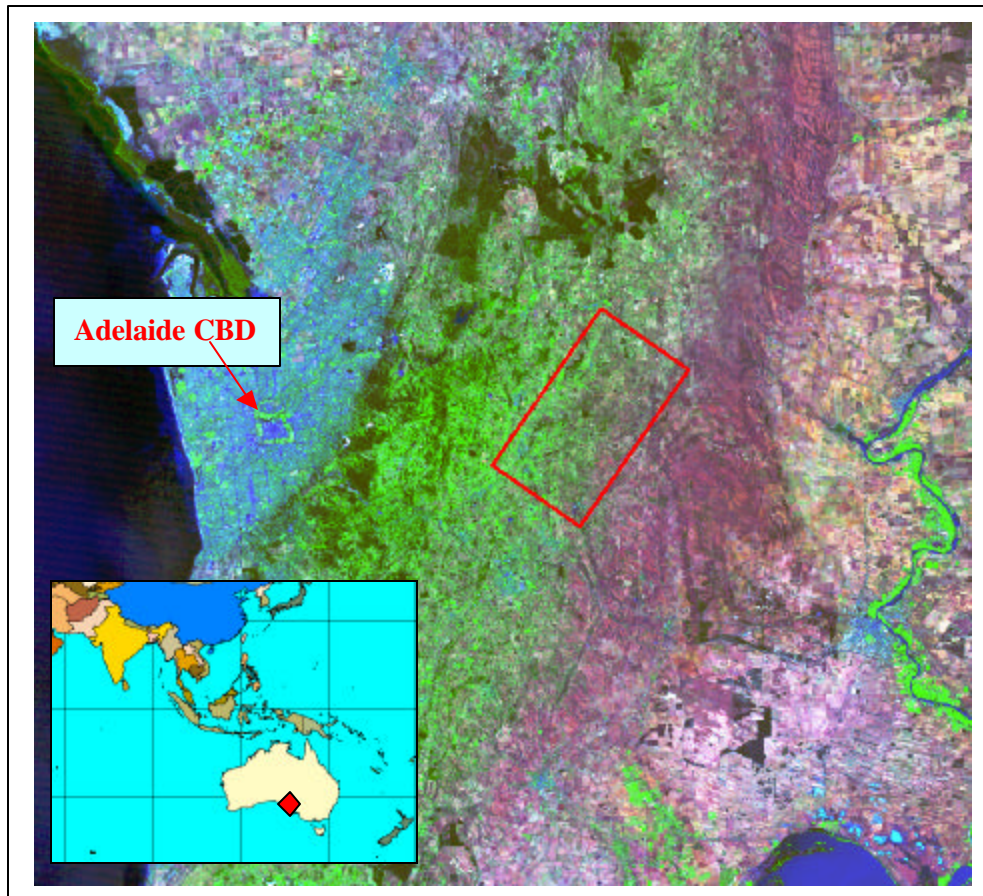


Figure 1: Study site (red rectangle) in the central Mount Lofty Ranges east of Adelaide, South Australia. Background image from Landsat ETM+ with bands 1,4,5 mapped to B,G,R (Summer 2000 data capture). Inset map shows location of site (red diamond) with respect to Australia and Asia.

Image acquisition in the 2000 AIRSAR flight over the Mount Lofty Ranges produced data in TOPSAR mode. In this product C band (5.6cm wavelength) HH and HV are used in interferometric SAR (IFSAR) production of a Digital Surface Model (DSM), leaving C band VV, L band (23cm wavelength) HH, VV and HV, and P band (68cm wavelength) HH, VV and HV for the bands constituting the TOPSAR imagery. This imagery is corrected to ground range and adjusted for topographic effects via the use of the coincident DSM from IFSAR. The acquisition occurred in the winter months of 2000 when the ground had high moisture content from winter rains. Summer 2000 imagery (VNIR, Panchromatic and Thermal) from ETM+ aboard Landsat was acquired and exposed strong differences between irrigated crops, pastures, native woodland, dry vegetation and bare soil (see Figure 1).

The research objective was to perform spectral classifications on each of the VNIR, TOPSAR and the combination of VNIR and TOPSAR image data. Ground truth was to be used for establishing training

data for supervised classification and additional ground truth used for creating accuracy assessments of all products.

METHODOLOGY

Radiometric adjustment of the VNIR image preceded the geometric correction to a common ground coordinate system. This radiometric adjustment included BDRF modelling using sun geometry and a 30m DEM, previously derived from topographic contour data. The DSM from TOPSAR was not used at this juncture as the model corresponded to the top of ground (where exposed) and either the top or near the top of vertical features such buildings and trees. Further processing of the DSM to produce a DEM is required. The image was then pan-sharpened using the higher spatial resolution panchromatic imagery simultaneously acquired with the VNIR data and resampled to 12.5m ground resolution. Geometric rectification was originally carried out to 1:50,000 digital map data using 85 ground control points (for the whole Landsat image) and a first order polynomial with total RMS of 16m.

The TOPSAR data was supplied in radiometrically calibrated dB using JPL pre and post flight calibration. Whilst the image data had already been corrected to ground range and for topographic geometry effects, the imagery still had to be adjusted to the common coordinate systems as that of the VNIR data. Again this was achieved using 1:50,000 digital map data using 39 Ground Control points with a total RMS of 13.1m. The major error in this rectification was the accuracy of the 1:50,000 maps. To improve this error new orthometric colour aerial imagery at 1.75m spatial resolution has been acquired and the geometric correction for both the VNIR and the TOPSAR imagery will be redone. Because the intention in this research was to merge the VNIR data with the TOPSAR data, the image rectification is a critical step. Errors of miss-registration may well produce distortions (particularly near the edge of objects) which may lead to errors in classification.

The spatial resolution of the two main images types used in this research are considerably different being approximately 30m and 5m for the ETM+ VNIR and TOPSAR data respectively. In order to make these two resolutions more compatible the ETM+ VNIR image was pan-sharpened using two methods; PCA forward-reverse resolution sharpening (ERDAS, 1999 and Chavez, 1991) and Smoothing Filter-based Intensity Modulation (SFIM) (Liu, 2000). The latter of these techniques proved to be superior in maintaining the spectral qualities of the VNIR image than the former. The original image data was supplied from the Australian Centre for Remote Sensing with 25m and 12.5m pixel resolutions for the VNIR and the panchromatic imagery respectively. Thus the pan-sharpened imagery was output at 12.5m spatial resolution with 6 multispectral bands. In re-sampling the 5m TOPSAR data to the common coordinate system, two images were output at 5m and 12.5m pixel resolutions. Both were subsequently used together with the 12.5 pan-sharpened VNIR imagery for combined classification processing.

Prior to classification the TOPSAR data was de-speckled used a Lee-sigma filter with a coefficient of variation computed for the image of 0.113, which compares well with the typical values expected from 16 look SAR. Figure 2 shows the VNIR and TOPSAR images prior to classification. Of note are the rural townships (A) in the south-west corner of the images showing strong blue tones in the VNIR image and strong backscatter in all three radar wavelengths. Native forests / woodland (B) exhibit lower infrared reflectance than that of irrigated crops and pastures but provide strong double or multiple bounce returns in all three radar wavelengths.

Ground truth for both the supervised classification and accuracy assessment was obtained from a combination of field visits over 6 month period from prior to the Landsat overpass to after the AIRSAR flight, land use polygon GIS data from the local Primary Industries and Resources (PIRSA) department and interpretation of the orthophoto imagery which was flown in March 2000. Supervised classification of both the VNIR and the TOPSAR data was performed using the Gaussian Maximum Likelihood (GML) algorithm. The use of this algorithm for radar is debatable and thus analysis of the normality of the SAR training data was performed. Because AIRSAR is acquired with 16 looks and with radar speckle predominantly removed, the training data showed strong tendency towards normality. For each information class multiple training samples were collected to ensure that the full spectral diversity of classes was collected. The same training sites were used for all three images and corresponded to the information classes shown in Table 1. This table also provides comments concerning spectral reflectance in VNIR and backscatter for the three radar wavelengths.

Consideration of the comments provided in Table 1 shows that there are likely to be errors of commission in a number of information classes for a single image type. For example, in the VNIR image

the spectral mixtures of grape vines with soil and shadow will most probably overlap with native trees along the edge of rural roads where again there is spectral mixing from the leaves of the eucalyptus and acacia trees with dry grass, soil and gravel roads. This confusion can be potentially resolved when examination to the radar backscatter of these information classes is considered. The posts in the vineyard trellis system potentially provide lower backscatter than that from larger tree trunks, particularly at L and P bands. Similarly, the irrigated pasture with strong infrared reflectance in the VNIR image potentially can overlap with vines when secondary plants are grown between the vine trellis systems. Again the SAR image potentially can resolve this situation with lower backscatter from the relatively smooth pasture surface, particularly at L and P band.

Following classification all thematic classification layers were thresholded using χ^2 distribution developed from the *posterior* probabilities derived in the GML classification algorithm. After inspecting the distributions of all

Information Class	VNIR Reflectance comments	SAR backscatter comments
Native woodland and forest	Characteristic vegetation response, but with lower IR reflectance than for crops and irrigated pasture.	Strong backscatter from tree trunks in all wavelengths. Some volume scattering from upper story branches and leaves at C Band HV. Some P band penetration to forest floor.
Irrigated grass pasture	Strong IR reflectance and red absorption.	Low response in all bands with response decreasing with increase in wavelength. No separability from dry pasture.
Buildings	Response strongest in the shorter wavelength bands, particularly visible blue. Weak reflectance in infrared.	Strong backscatter at all wavelengths with double bounce off vertical building sides. Similar to some backscatter from trees.
Conifers and pines	Similar reflectance to native woodland, but darker in most bands due to tree density and shadows.	Similar response to native vegetation. However the cross-polarized return is different to that of native vegetation, probably due to differing branch patterns.
Dry grass pasture with some exposed soil Quarry (open cut)	Bright reflectance at all wavelengths with strongest values in middle infrared (soil) Very strong reflectance from exposed rocks and soil.	Low response in all bands with response decreasing with increase in wavelength. Poor separability from irrigated pasture. Bright return from quarry sides facing radar. Considerable radar shadow in other places.
Grape vines	Green vine leaves, soil between the vine rows and shadow make this reflectance a genuine mixture. Confusion exists between this class and native trees scattered along road edges.	The dominant backscatter is from the wooden posts and, when close to parallel with radar antenna, the wire supports for the vines. Backscatter decreases with wavelength.
Dam water	A poor reflector with decreasing response with wavelength. Edge pixels show strong mixing.	A smooth surface generating a very low backscatter at all wavelengths.

Table 1: Information classes used for land cover classification.

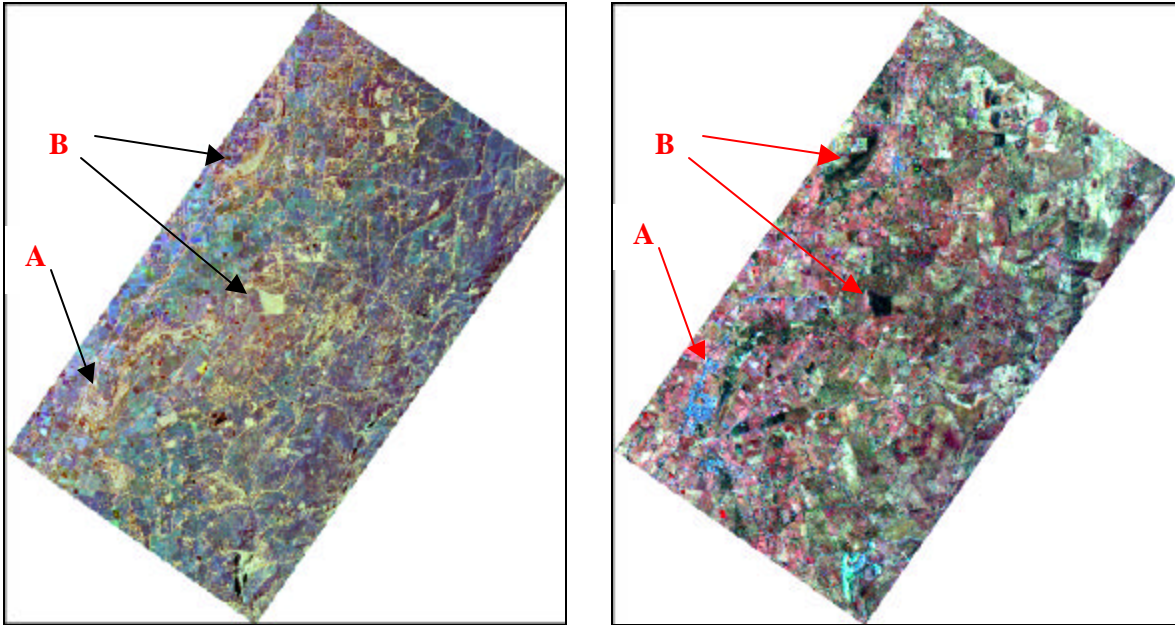


Figure 2: Left - TOPSAR image after geometric rectification and de-speckling (R,G,B - Pw, Lw, Cv) Right – VNIR image after pan-sharpening (SFIM) and rectification (R,G,B – 5,3,1)

classes, the χ^2 distance was set to correspond to a 1% rejection. Accuracy checks followed via the use of stratified random sampling using 160 checkpoints, using points wherein the selected raster cell was one of a majority in a 3 x 3 neighbourhood. The stratified random selection was constrained to a minimum of 10 checkpoints per information class. Kappa statistics and accuracy percentages were computed as a total and for each information class.

IMAGE FUSION

In the fusion of the VNIR and SAR images consideration was given to the radically different data types with the original VNIR data being integer DN from 0 - 255 and the SAR data being floating point decibels from +51 dB to - 332 dB. In order to ensure that the data ranges of the two images were more compatible prior to fusion, each data value was transformed to one representing its distance from the band mean in terms of the standard deviation of that band. That is:

$$DV_i^T = (G_i - DV_i) / G_i \dots\dots\dots(1)$$

Where, DV_i^T = transformed data value in band i, DV_i = existing data value in band i, G_i = global mean for band i G_i = global standard deviation for band i.

Following this transformation the two images were simply combined into one image with 13 layers; layers 1 – 6 for the VNIR bands and layers 7 – 13 for the C, L and P bands. Figure 3 illustrates the improvement in image detail via the combination of near infrared (VNIR band 4) with the Cv and Lv bands from TOPSAR. Note the additional detail in the township (T) where trees and buildings are better discriminated and the additional details in the irrigated pasture (P) and vines (V).

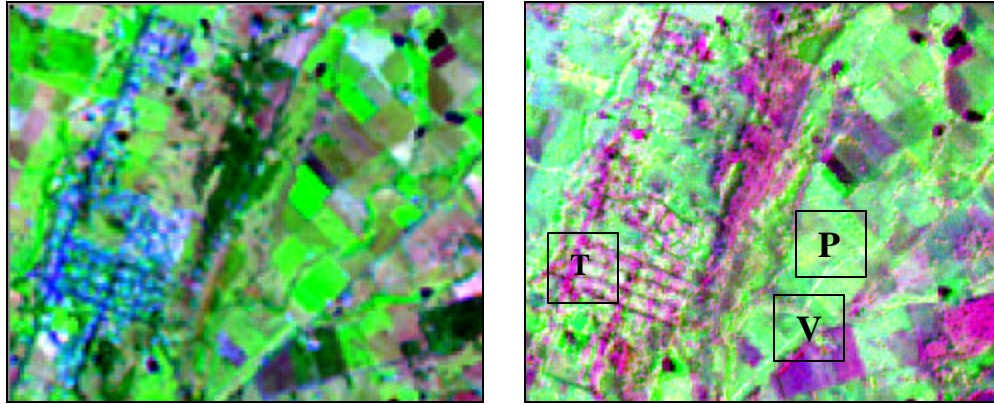


Figure 3: Comparison of enlarged images showing detail around a rural town (Woodside)
 Left – Bands 1,4,5 (B,G,R) for VNIR image. Right – Cvv , VNIR band 4, Lvv (B,G,R) for the combined images.

RESULTS

Information Class	Kappa Statistics			
	VNIR (all bands)	TOPSAR (all bands)	VNIR + TOPSAR C and L bands	VNIR + TOPSAR (all bands)
Native woodland and forest	0.4286	0.6491	0.7932	1.0000
Irrigated grass pasture	0.4359	0.2958	0.8089	0.8747
Buildings	1.0000	0.2982	0.4763	0.4063
Conifers and pines	-0.0256	0.2564	0.2994	0.3846
Dry grass pasture / exposed soil	0.4667	0.8148	0.8597	1.0000
Quarry (open cut)	0.0127	0.1007	0.0895	-0.0127
Grape vines	0.1903	0.0789	0.2776	0.2870
Dam water	0.7621	1.0000	0.7995	0.8222
Overall Kappa Statistic	0.2724	0.3961	0.5627	0.6181
Overall Classification accuracy %	42.50	61.25	67.19	70.00

Table 2: Accuracy statistics for the classification of VNIR, TOPSAR and combinations of VNIR and TOPSAR

Table 2 summarizes the accuracy statistics for various images and combinations of images / bands. The overall accuracy statistics are relatively low compared with typically published values, but represent the realistic accuracies when genuine random accuracy assessment is undertaken. The lower than expected overall accuracies are possibly also in part due to registration errors between the two images. On a number of samples test points near the edge of features such as forests, errors were noted due to mixing of slightly miss-registered images. The kappa statistics for the individual classes showed a serious problem with the quarry class and less than the expected quality for the Grape Vine class, given the success reported by Bruce (2000). Visual comparison of the classifications from the VNIR and the combined VNIR and TOPSAR with each other and with land use maps indicated better results than Table 2 suggests. An example of this comparison is illustrated in Figure 4, which presents an enlargement of a section in the east of the study site with a small town (Charleston), grape vines, irrigated pastures and some native forest classes. In Figure 4 left there are strong indications of over classification of vines when compared with the vector land use map (Figure 4, centre). There is an improvement in this class in Figure 4 (right).

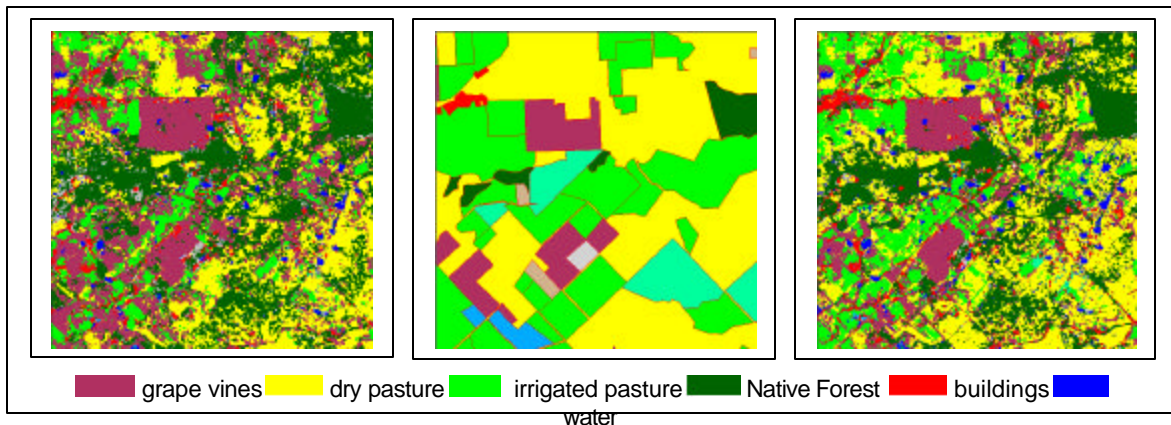


Figure 4: Comparison of classifications showing detail around a rural town (Charleston)
 Left – Classified VNIR image. Centre – Vector land use map. Right – Classified combination of VNIR and TOPSAR images (all bands).

Table 2 demonstrates that classification accuracy generally improves with the addition of SAR imagery to VNIR imagery, with the most useful contributions from C and L band with P band having less influence on the classification accuracies. This can be attributed to P band exhibiting a considerably lower dynamic range than C and L bands for the AIRSAR instrument and because at the 68cm wavelength of P band, there will be penetration through crops, and forest canopies. It was expected that P band would contribute more significantly to the differentiation of buildings from trees, but this was less successful than anticipated.

CONCLUSIONS

The preliminary research reported in this paper supports the hypothesis that improvement in classification accuracy can occur when VNIR imagery is combined with multi-spectral SAR imagery. Significant issues exist with the combination of these types of data with image geometry and accurate co-registration being very important. The different spatial resolutions of the two data sets used in this paper also provided challenges, which were not completely resolved. Alternative classification algorithms such as image segmentation and rule-based classification may well improve the levels of accuracy. The paper provides sufficient impetus for the continued examination of the combination of satellite VNIR images with satellite SAR images, particularly with the advent of EVNISAT ASAR with dual polarization at C band and, in the future, ALOS PALSAR with quad polarization at L band.

ACKNOWLEDGEMENTS

My thanks go to my CSIRO Land and water, CRC LEME (Dr. Ian Tapley), the University of Adelaide and to my research group (SMIG) at the University of South Australia for funding support for the PACRIM mission in Adelaide in 2000. I also thank Dr. A. Forghani and those University students who assisted in the collection of data.

REFERENCES

- Bruce, D.A., P. Davies and R. Fitzpatrick, 1999.** *Validating Soil Moisture Estimates from Polarimetric Radar Using GIS Models: further results from the 1993 AIRSAR mission to Australia.* PACRIM AIRSAR Significant Results Workshop, Maui, Hawaii, 24 – 24 August, 1999.
- Bruce, D.A., 2000.** *Vegetation Discrimination using L Band Radar and Visible Infrared Imagery*, in proceedings of the 10th Australasian Remote Sensing and Photogrammetry Conference, Adelaide, Australia, August.
- Chavez, P. S. Jr., et al, 1991.** *Comparison of Three Different Methods to Merge Multiresolution and Multispectral Data: Landsat TM and SPOT Panchromatic.* Photogrammetric Engineering & Remote Sensing, Vol. 57, No. 3: 295-303.
- ERDAS, 1999.** ERDAS Field Guide, 5th Edition, ERDAS Inc., Atlanta, Georgia, USA.

Lui, J.G., 2000. Smoothing Filter-based Intensity Modulation: a spectral preserve image fusion technique for improving spatial details. *International Journal of remote Sensing*, Vol. 21, No. 18: 3461 – 3472.